



1 **Refined mapping of tree cover at fine-scale using time-series**
2 **Planet-NICFI and Sentinel-1 imagery for Southeast Asia (2016-**
3 **2021)**

4 Feng Yang^a, Zhenzhong Zeng^{a,*}

5 ^a School of Environmental Science and Engineering, Southern University of Science and Technology,
6 Shenzhen 518055, China

7

8

9 * Correspondence to: zengzz@sustech.edu.cn (Zhenzhong Zeng)

10 Mailing Address:

11 College of Engineering N808

12 Southern University of Science and Technology

13 Shenzhen, China

14

15

16

17 The manuscript for *Earth System Science Data*

18 April 25, 2023

19



20 **Abstract:**

21 High-resolution mapping of tree cover is indispensable for effectively addressing tropical forest carbon loss,
22 climate warming, biodiversity conservation, and sustainable development. However, the availability of
23 precise high-resolution tree cover map products remains inadequate due to the inherent limitations of
24 mapping techniques utilizing medium-to-coarse resolution satellite imagery, such as Landsat and Sentinel-2
25 imagery. In this study, we have generated an annual tree cover map product at a resolution of 4.77 m for
26 Southeast Asia (SEA) for the years 2016-2021 by integrating Planet-Norway's International Climate &
27 Forests Initiative (NICFI) imagery and Sentinel-1 Synthetic Aperture Radar data. we have also collected
28 annual samples to assess the accuracy of our Planet-NICFI tree cover map products. The results show that
29 our Planet-NICFI tree cover map products during 2016-2021 achieve high accuracy, with an overall accuracy
30 of $\geq 0.867 \pm 0.017$ and a mean F1 score of 0.921, respectively. Furthermore, our tree cover map products exhibit
31 high temporal consistency from 2016 to 2021. Compared to existing map products (FROM-GLC10, ESA
32 WorldCover 2020 and 2021), our tree cover map products exhibit better performance, both statistically and
33 visually. Yet, the imagery obtained from Planet-NICFI performs less in mapping tree cover in areas with
34 diverse vegetation or complex landscapes due to insufficient spectral information. Nevertheless, we highlight
35 the capability of Planet-NICFI datasets in providing quick and fine-scale tree cover mapping to a large extent.
36 The consistent characterization of tree cover dynamics in SEA's tropical forests can be further applied in
37 various disciplines. The annual Planet-NICFI V1.0 tree cover map products from 2016 to 2021 at 4.77 m
38 resolution are publicly available at <https://cstr.cn/31253.11.sciencedb.07173> (Yang and Zeng, 2023).

39

40 **1 Introduction**

41 Forests and tree-based systems outside forests play a crucial role in land-based carbon emissions or removals,



42 making them essential for supporting and monitoring the implementation of the Reducing Emissions from
43 Deforestation and Forest Degradation (REDD+) and other land-based activities under the Paris Agreement
44 (Skea et al., 2022; CoP26, 2021; FAO, 2020). However, current forest cover map products exhibit significant
45 errors in accurately estimating forest area and change, particularly in areas such as trees outside forests and
46 forest edge landscapes (Mugabowindekwe et al., 2023; Reiner et al., 2022; Brandt et al., 2020). As a result,
47 there is a growing demand for timely, high-quality, and high-resolution tree cover products to accurately
48 capture the dynamics and changes in tree cover.

49

50 Many tree cover maps have been developed at medium-to-coarse resolutions (10-500 m), such as Finer
51 Resolution Observation and Monitoring of Global Land Cover 10 m (FROM-GLC10; Gong et al., 2019),
52 Environmental Systems Research Institute (ESRI) Land Cover (2017-2021) (Karra et al., 2021), European
53 Space Agency (ESA) WorldCover 2020 and 2021 (Zanaga et al., 2022; Zanaga et al., 2021), GFC (Hansen et
54 al., 2013), Globeland30 (Chen et al., 2015), Copernicus Global Land Service (CGLS) Land Cover (Buchhorn
55 et al., 2020), ESA Climate Change Initiative (CCI) (ESA, 2017) and the National Aeronautics and Space
56 Administration (NASA) MCD12Q1 (Friedl and Sulla-Menashe, 2019). However, accurate high-resolution
57 tree cover maps at continental-to-global scales are still lacking due to mapping through medium-to-coarse
58 resolution imagery (Zanaga et al., 2021; Hansen et al., 2010). Consequently, some uncertainties occur in
59 acquiring global tree inventories and monitoring forest disturbances (deforestation and forest degradation).
60 This is mainly due to isolated trees or long narrow forest cover removal (Reiner et al., 2022; Wagner et al.,
61 2022; Sexton et al., 2016; Hammer et al., 2014; Hsieh et al., 2001).

62

63 Only recently have two tree cover maps at <4.77 m from preprints been produced over Africa and the state



64 of Mato Grosso in Brazil using Planet-Norway's International Climate & Forests Initiative (NICFI) imagery
65 based on deep learning (Wagner et al., 2023; Reiner et al., 2022). However, these two maps have only limited
66 temporal or spatial coverage that occurred. Since the early 21st century, agricultural expansion has created a
67 new wave of drastic land use/land cover changes in Southeast Asia (SEA), leading the region to be one of the
68 most deforested regions worldwide (Zeng et al., 2018a; Zeng et al., 2018b; Achard et al., 2014). Average
69 elevations and slopes of forest loss sites have significantly increased in SEA, particularly in the 2010s,
70 geometrically irregular upland land use sites commonly occur (Velasco et al., 2022; Feng et al., 2021).
71 However, existing tree cover maps have underestimated deforestation (25-116%) and upland agricultural
72 expansion rates (9-113%), especially on the topographic boundaries in SEA (Zeng et al., 2018a). Thus, fine-
73 resolution tree cover maps in SEA, with high spatial resolution and longer consistent time series, are urgently
74 needed to accurately monitor tree cover loss and related illegal deforestation. In addition, combining high-
75 resolution optical imagery and Synthetic Aperture Radar (SAR) data (Sentinel-1) to produce large-area tree
76 cover maps is still in its early stage (Zanaga et al., 2022; Karra et al., 2021; Zanaga et al., 2021; Buchhorn et
77 al., 2020; Hansen et al., 2010).

78

79 Concurrently, advances in large-scale cloud computing (e.g., Google Earth Engine, GEE; Gorelick et al.,
80 2017) and available high-resolution satellite imagery (Roy et al., 2021) can facilitate the development of
81 high-resolution and longer time-series tree cover maps at continental-to-global scales. In this paper, we
82 generated state-of-the-art fine-scale open-source tree cover maps for SEA during 2016-2021 using Planet-
83 NICFI imagery, Sentinel-1 SAR data, and the random forest (RF) method from a previous study (Yang et al.,
84 2023). This dataset allows for extensive assessments of forest dynamics change, such as deforestation, forest
85 degradation, and reforestation. In addition, our dataset can monitor trees outside forests and long narrow



86 forest cover removal, thus improving the accuracy of automated continental tree inventories, which help
87 optimize REDD+ under the Paris Agreement.

88

89 **2 Materials and method**

90 **2.1 Satellite imagery**

91 We utilized Planet-NICFI and Sentinel-1 imagery for the years 2016-2021 to generate time series tree cover
92 maps for SEA. The Planet-NICFI program provides high-resolution (4.77 m per pixel) optical PlanetScope
93 surface reflectance mosaics specifically designed for the tropics. These mosaics offer accurate and reliable
94 spatial data with minimized effects from atmosphere and sensor characteristics, making them an ideal 'ground
95 truth' representation (Planet Team, 2017). The mosaics cover the best imagery to represent every part of the
96 coverage area during leaf-on periods from June to November based on cloud cover and acutance (image
97 sharpness). The Planet-NICFI imageries consist of four bands: red, green, blue, and near-infrared, and cover
98 a time period from 2015 to 2020 at bi-annual resolution for the archive, and from 2020 to 2023 at monthly
99 resolution for monitoring purposes. We accessed and utilized these products in the GEE platform by
100 authorizing our NICFI account to the GEE account.

101

102 We utilized Sentinel-1 on the GEE platform, specifically the 10 m resolution dual-polarization Ground Range
103 Detected (GRD) scenes (VV + VH). We chose Sentinel-1 SAR imagery to correct cases of overestimation
104 caused by confusion with herbaceous vegetation, or underestimation due to optical satellite observations
105 omitting deciduous or semi-deciduous characteristics (Shimada et al., 2014). The SAR imagery, available
106 every 12 days for a single satellite or 6 days for a dual-satellite constellation from October 2014 to the present,
107 was pre-processed with the Sentinel-1 Toolbox for thermal noise removal, radiometric calibration, and terrain



108 correction.

109

110 **2.2 Validation dataset collection**

111 We collected other validation datasets to assess the tree cover products during 2016-2021, except for 2019.

112 Our mapping approach (Lang et al., 2022) has been tested after being developed in 2019. However, we were

113 unable to obtain suitable validation datasets to investigate the accuracy of our time-series tree cover datasets

114 because existing samples mainly have coarse resolutions (e.g., ≥ 10 m). This can cause significant

115 uncertainties in assessing high-resolution tree cover maps.

116

117 Thus, following Yang et al. (2023), we randomly generated 1,515 points to ensure the representativeness of

118 collected visual samples (Fig. 1). Then, these points were labeled these points as forests or non-forests by

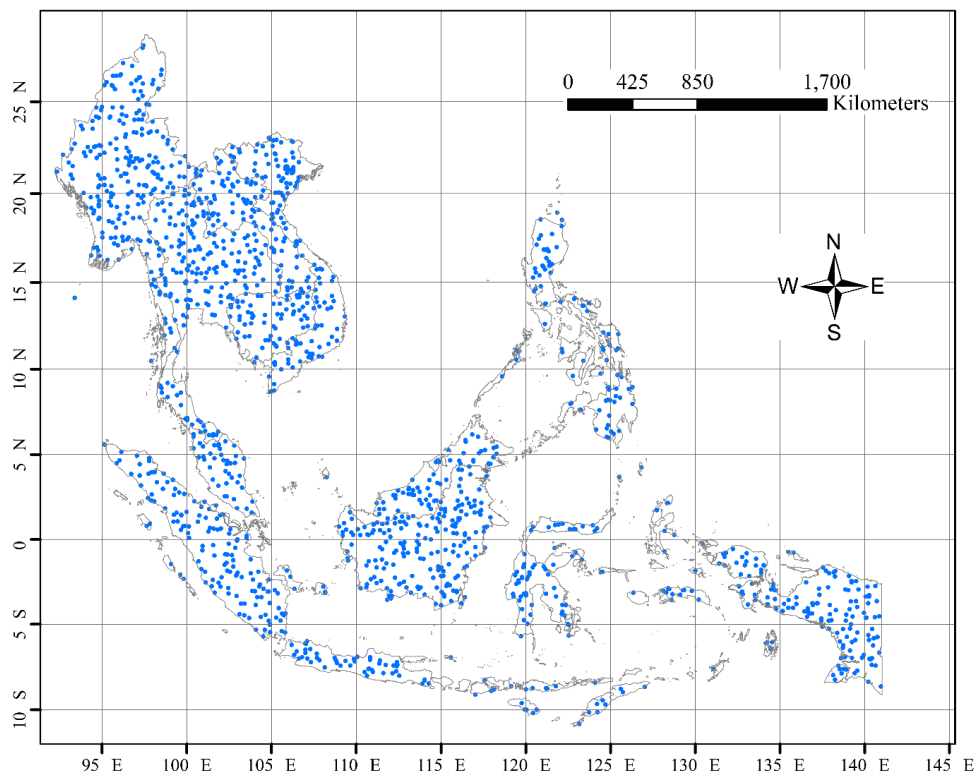
119 four human interpreters using Planet Explorer of QGIS. During labeling, we fixed the location of the 1,515

120 points and changed the year of the Planet-NICFI imagery. The labels included 2016, 2017, 2018, 2020, and

121 2021. In addition, we overlapped the 10 m tree height data of Lang et al. (2022) over the Planet-NICFI

122 imagery to ensure that the labels met the tree height criteria (i.e., ≥ 5 m). Detailed information on the

123 validation dataset is listed in Table 1.



124

125

Figure 1 Spatial distribution of randomly generated 1,515 validation dataset points.

126

127

Table 1 Information of the mapped validation dataset for evaluating the generated tree cover products.

Period	Count of sample points		
	Forest	Non-forest	Total
2016	1,086	429	1,515
2017	1,126	389	1,515
2018	977	538	1,515
2020	1,093	422	1,515
2021	952	563	1,515

128

129 **2.3 Method**

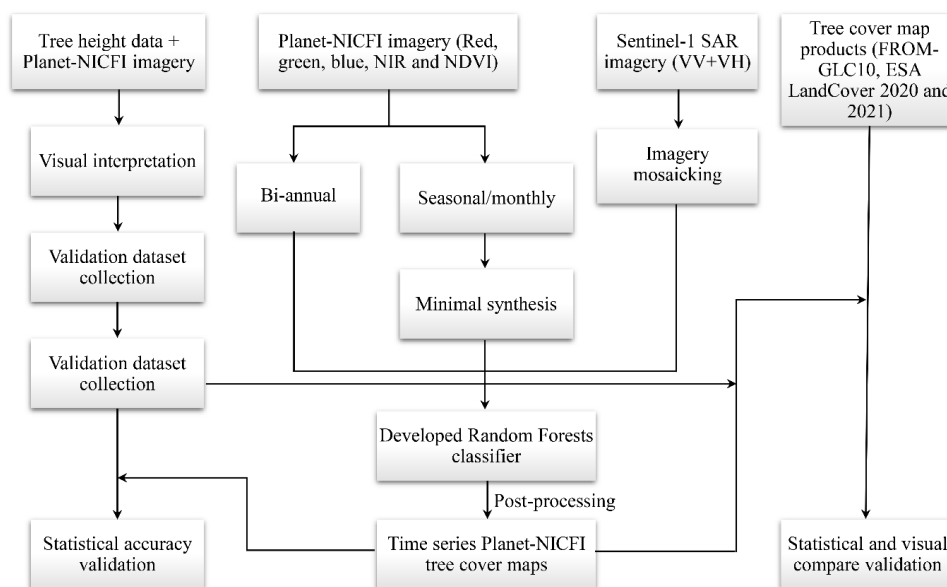
130 We integrated Planet-NICFI and Sentinel-1 SAR imagery to generate a high-resolution (4.77 m) annual tree

131 cover map product for SEA covering the years 2015-2021. Our framework involved several key steps,



132 including defining mapped objects, preprocessing of imagery, and generation of time-series tree cover maps.

133 The detailed workflow is illustrated in Fig. 2.



134

135 **Figure 2** Workflow of generating tree cover products for 2016-2021, including imagery preprocessing,
136 generation of tree cover maps, and accuracy validation.

137

138 2.3.1 Definition of mapped objects

139 Traditionally, forests are considered to meet specific criteria (tree cover and height). For example, the Food
140 and Agriculture Organization (FAO) of the United Nations defines forests as land spanning more than 0.5
141 hectares with trees higher than 5 m and a canopy cover above 10% (FAO, 2020). According to the United
142 Nations Framework Convention on Climate Change (UNFCCC), forests are defined as areas with a minimum
143 canopy cover of 10-30%, minimum tree height of 2-5 m, and a minimum area of 0.1 ha (Parker et al., 2008).
144 In this study, we utilized Planet-NICFI imagery to generate a prototype map with a resolution of 4.77 m. Our
145 tree cover map products serve as baseline data for forest cover analysis. Upon further development of the
146 map to include trees higher than 5/2-5 m, it can be utilized for deriving forest maps for various functions,



147 such as those provided by FAO and UNFCCC.

148

149 2.3.2 Preprocessing of imagery

150 We utilized the GEE platform to process Planet-NICFI imagery and Sentinel-1 SAR data to generate tree
151 cover products for the years 2016-2021 (Fig. 2). Following the methodology of Yang et al. (2023), we
152 employed the `ee.ImageCollection.mosaic()` function to merge and assemble overlapping Sentinel-1 SAR data
153 over the specified time period into a seamless, continuous imagery. Subsequently, we performed bilinear
154 resampling on the SAR imagery, specifically the VV and VH bands, to obtain a high-resolution tree cover
155 map with a spatial resolution of 4.77 m.

156

157 Planet-NICFI offers imagery at two different temporal frequencies spanning from 2016 to 2021. This includes
158 semi-annual imagery from 2016 to 2019 and monthly data from 2020 to 2021. To create a coherent and
159 consistent dataset for 2020 and 2021, we synthesized the selected time window of monthly imagery into
160 single imagery for each band, namely red, green, blue, and near-infrared bands. Specifically, we utilized the
161 `ee.ImageCollection.min()` function on each monthly imagery to extract the minimum monthly imagery, which
162 was then used to generate the second semi-annual imagery for 2020 and 2021. This approach was employed
163 to minimize the impact of cloud pollution on Planet-NICFI imagery (Oishi et al, 2018).

164

165 2.3.3 Generation of time-series tree cover maps

166 In addition to applying the RF approach in our tree cover mapping (Yang et al., 2023), RF-based methods
167 have been widely employed to develop global land cover and land use (LCLU) products and show good
168 performance (Zanaga et al., 2022; Zanaga et al., 2021; Buchhorn et al., 2020). To obtain our time-series tree



169 cover datasets, we combined our RF approach using GEE with a cloud machine learning platform to obtain
170 semi-annual Planet-NICFI and Sentinel-1 imageries for years 2016-2021 (Fig. 2). We then conducted various
171 postprocessing to generate tree cover products for SEA, including downloading from a cloud platform to a
172 local location, mosaic, clip, projection, and correlation statistics.

173

174 **2.4 Statistical accuracy assessment**

175 We used two methods to assess the statistical accuracy of our tree cover maps. We first used the confusion
176 matrix to calculate the user's accuracy, producer's accuracy, and overall accuracy at a 95% confidence level
177 (Olofsson et al., 2014) and the F1 score. Then, following Tsendbazar et al. (2021), we used a stability index
178 based on the user's and producer's accuracy to evaluate the time-series accuracy consistency of the tree cover
179 product. The stability index used to evaluate tree cover accuracy is expressed as

$$SI_{t1} = \frac{|TC_{t1} - TC_{t1-1}|}{TC_{t1-1}} \times 100 \quad (1)$$

180 where SI_{t1} is the stability index that indicates the accuracy of tree cover maps (user's or producer's accuracy)
181 at time $t1$, TC_{t1} is tree cover accuracy at time $t1$ and TC_{t1-1} is tree cover accuracy at the previous time ($t0$
182 or the reference year). We also used the maximum and average stability index for two consecutive years to
183 assess the stability of our tree cover products over a long period.

184

185 **3 Results**

186 We employed two approaches to assess the performance of our Planet-NICFI 2016-2021 tree cover map
187 products. Firstly, we estimated the accuracy of our tree cover products for each year to gain insights into their
188 accuracy and consistency, based on a study by Tsendbazar et al. (2021). Secondly, we compared our tree
189 cover products to widely used global tree cover products at 10 m resolution, including FROM-GLC10 in



190 2017 (Gong et al., 2019), as well as ESA WorldCover 2020 and 2021 (Zanaga et al., 2022; Zanaga et al.,
191 2021).

192

193 3.1 Statistical accuracy assessment

194 We reported the annual accuracy of the time-series Planet-NICFI tree cover map product in Table 2 with a
195 95% confidence level. The results for 2019 were provided by Yang et al. (2023). The overall accuracy of the
196 tree cover map product ranged between $0.867\text{-}0.907 \pm 0.015$ from 2016 to 2021, with the highest accuracy
197 of 0.907 ± 0.014 in 2021 and the lowest accuracy of 0.867 ± 0.017 in 2016 (Table 2). This discrepancy could
198 be due to poor data in the Planet-NICFI imagery during 2016. The F1 score showed a similar trend from 2016
199 to 2021, with an average of approximately 0.921. The user's accuracy consistently exceeded 0.901 ± 0.017
200 over the six years, except for 2016 when it was 0.862 ± 0.021 . The producer's accuracies were all higher than
201 0.912 ± 0.014 (Table 2). Nevertheless, the mapping results of our time-series Planet-NICFI tree cover map
202 products were highly consistent. Additionally, compared to the tree cover, the non-tree cover showed lower
203 user's accuracy, producer's accuracy, and F1 score (i.e., approximately 0.856 ± 0.027 , 0.852 ± 0.025 , and 0.853,
204 respectively), likely due to the complex composition of non-tree cover types, such as shrubland and
205 herbaceous wetland.

206

207 **Table 2** User's accuracies, producer's accuracies, F1 score, and overall accuracies of the Planet-NICFI V1.0
208 2016-2021 tree cover maps for SEA at a 95% confidence level. The accuracy evaluation results in 2019 were
209 provided by Yang et al. (2022)²⁵.

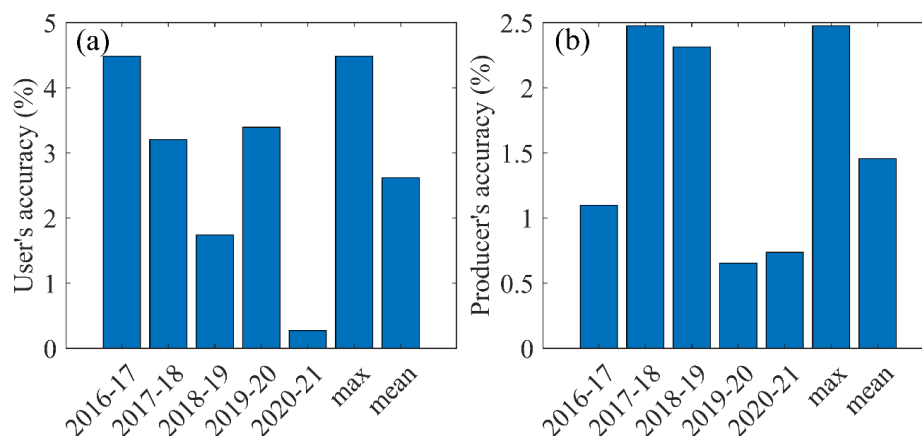
Year	Classification	User's accuracy	Producer's accuracy	F1 score	Overall accuracy
2016	Tree cover	0.862 ± 0.021	0.925 ± 0.018	0.892	0.867 ± 0.017
	Non-tree cover	0.876 ± 0.031	0.783 ± 0.026	0.827	
2017	Tree cover	0.901 ± 0.017	0.935 ± 0.016	0.917	0.892 ± 0.016
	Non-tree cover	0.874 ± 0.033	0.814 ± 0.027	0.843	
2018	Tree cover	0.929 ± 0.016	0.912 ± 0.014	0.920	0.892 ± 0.015
	Non-tree cover	0.816 ± 0.033	0.85 ± 0.030	0.832	



2019	Tree cover	0.913±0.012	0.933±0.010	0.923	0.895±0.011
	Non-tree cover	0.857±0.022	0.819±0.021	0.837	
2020	Tree cover	0.944±0.014	0.927±0.011	0.935	0.900±0.014
	Non-tree cover	0.754±0.041	0.803±0.040	0.778	
2021	Tree cover	0.947±0.014	0.934±0.011	0.940	0.907±0.014
	Non-tree cover	0.778±0.038	0.816±0.039	0.796	

210

211 We also estimated the stability of our Planet-NICFI tree cover map accuracy over 2016-2021 (Fig. 3). The
 212 results show that the user's and producer's stability indexes were low than 4.5% and 2.5%, respectively,
 213 indicating the good stability of our mapped Planet-NICFI tree cover map for the six years (2016-2021).



214

215 **Figure 3** Stability index estimates for the Planet-NICFI tree cover map product 2016-2021: the stability index
 216 for (a) the user's accuracy and (b) the producer's accuracy.

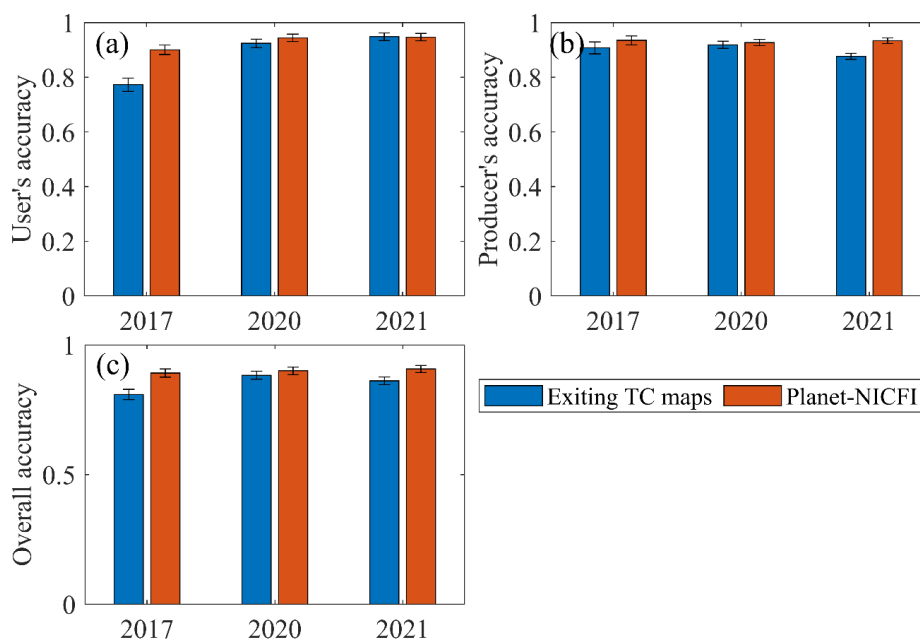
217

218 3.2 Comparison with existing tree cover products

219 We compared our mapped Planet-NICFI tree cover map with FROM-GLC10, ESA WorldCover 2020 and
 220 2021 regarding statistical accuracy (Fig. 4). The results show that our tree cover map outperformed FROM-
 221 GLC10 in user's accuracy, producer's accuracy, and overall accuracy. The user's accuracy and overall
 222 accuracy of our tree cover map exceeded 0.083. ESA WorldCover 2020 and 2021 showed similar
 223 performances to our Planet-NICFI tree cover map. Particularly, the user's accuracy, producer's accuracy, and
 224 overall accuracy of ESA WorldCover 2020 decreased by 0.020, 0.008, and 0.017, respectively (Fig. 4). This



225 may be because we all used the SAR imagery as input and applied the RF-based machine learning method to
226 classify our tree cover.



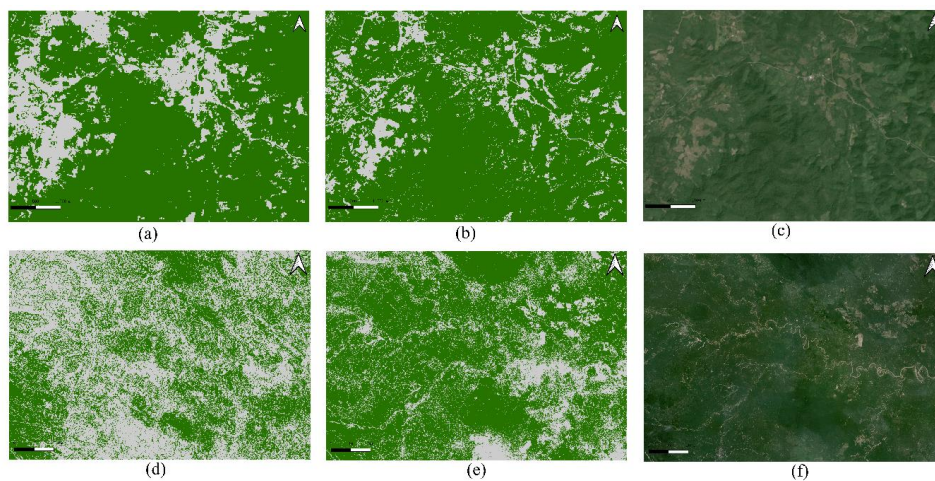
227
228 **Figure 4** Accuracy comparison between existing tree cover maps and the generated Planet-NICFI tree cover
229 map at a 95% confidence level: (a) user's accuracy, (b) producer's accuracy, and (c) overall accuracy.

230

231 We selected six locations (three mainland SEA areas and three maritime SEA areas) to visually compare our
232 Planet-NICFI tree cover maps with three other 10-meter products, namely, FROM-GLC10, ESA WorldCover
233 2020 and 2021 (Figs. 5-7). In comparison, it is easier for FROM-GLC10 to classify all mixed tree and non-
234 tree areas into non-tree cover maps (Fig. 5a). This may be because FROM-GLC10 cannot apply SAR imagery
235 to tree cover mapping. However, ESA WorldCover 2020 and 2021 can capture tree cover landscapes at a
236 higher level of detail than FROM-GLC, such as long narrow roads, croplands, and built-up areas (Figs. 6-
237 7a). It should be noted that ESA WorldCover 2020 and 2021 omitted some long narrow non-tree cover
238 landscapes and small isolated tree cover and non-tree cover landscapes due to the limitation of the imagery



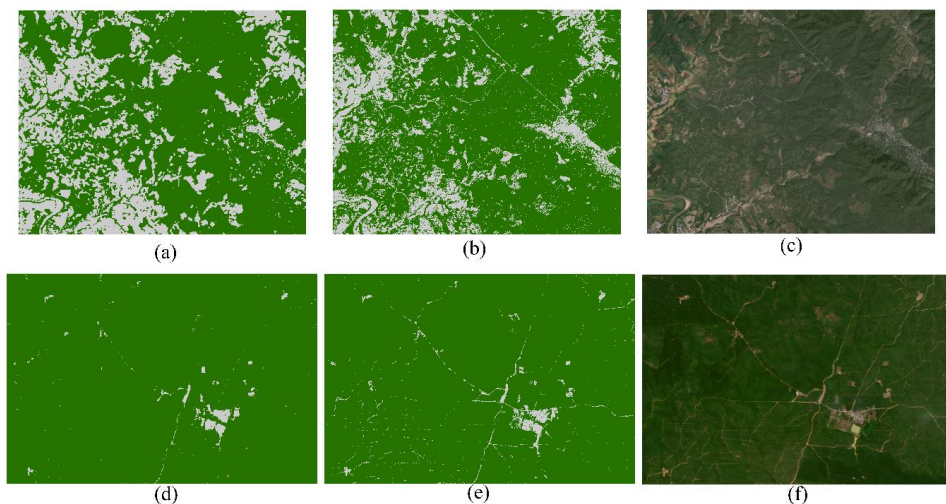
239 resolution (10 m).



240

241 **Figure 5** Comparison of FROM-GLC10 (a) and (d), Planet-NICFI tree cover (b) and (e), and Planet-NICFI
242 imagery (c) and (f) for mainland SEA area (101.594°-101.651°E, 19.254°-19.294°N; top row) and maritime
243 SEA area (101.925°-103.296°E, -2.096°-1.145°S; bottom row). Green and gray 20% indicate tree cover and
244 non-tree cover, respectively.

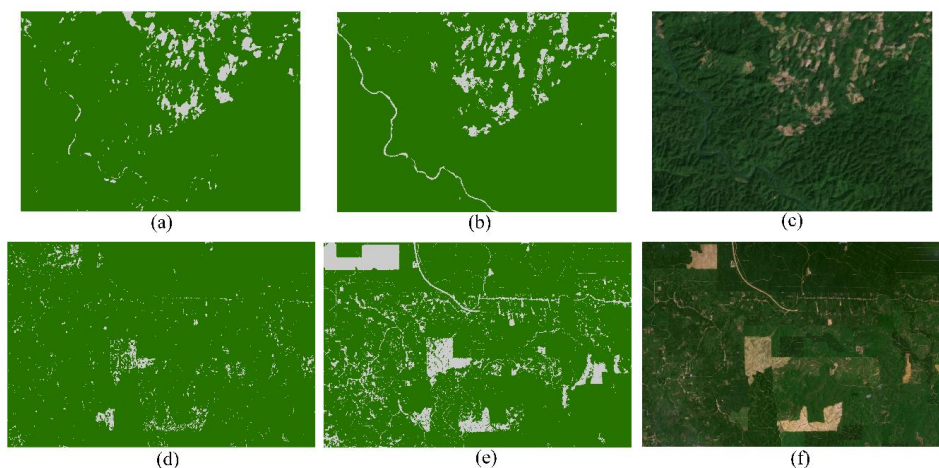
245



246

247 **Figure 6** Comparison of ESA WorldCover 2020 (a) and (d), Planet-NICFI tree cover (b) and (e), and Planet-
248 NICFI tree cover (b) and (e), and Planet-NICFI imagery (c) and (f) for mainland SEA area (98.310°-98.392°E, 17.102°-17.166°N; top row) and
249 maritime SEA area (99.983°-100.064°E, 1.387°-1.442°N; bottom row). Green and gray 20% indicate tree cover and non-tree cover, respectively.

250
251



252

253 **Figure 7** Comparison of ESA WorldCover 2021 (a) and (d), Planet-NICFI tree cover (b) and (e), and Planet-
254 NICFI imagery (c) and (f) for Mainland SEA area (102.179°-102.249°E, 18.676°-18.726°N; top row) and
255 maritime SEA area (99.951°-100.063°E, 1.892°-1.967°E; bottom row). Green and gray 20% indicate tree
256 cover and non-tree cover, respectively.

257

258 **4 Discussion**

259 Our time-series Planet-NICFI tree cover products were mapped twice a year to mitigate the impact of smog,
260 light, cloud, and topographic effects in tropical areas (Roy et al., 2021; Marta et al., 2018). These high-
261 resolution tree cover products meet the minimum tree height requirement of ≥ 5 m. However, it should be
262 noted that we cannot guarantee 100% tree cover for each higher-resolution pixel, which may introduce some
263 uncertainties when using the higher-resolution tree cover map. Despite excluding plantations during sample
264 point labeling, some plantations, such as oil palm, may still be mixed into our tree cover products due to
265 similarities in anomalies (Mugabowindekwe et al., 2023; Zanaga et al., 2022; Zanaga et al., 2021). As a result,
266 caution should be exercised when using our Planet-NICFI tree cover products for certain purposes.

267

268 To generate high-resolution time series tree cover map products at a continental scale, we utilized advanced
269 random forests machine learning algorithms on the platform. However, for fine-scale tree cover mapping,



270 deep learning-based segmentation methods, such as U-net, are necessary, particularly when using limited
271 bands (Mugabowindekwe et al., 2023; Wagner et al., 2023; Zanaga et al., 2022; Zanaga et al., 2021; Brandt
272 et al., 2020). As a result, our tree cover map products still have some uncertainty due to limitations in the
273 optical PlanetScope imagery. To improve our tree cover mapping product with higher resolution, we may
274 need to consider adding more bands or utilizing advanced deep learning algorithms in the future.

275

276 **5 Data availability**

277 The high-resolution Planet-NICFI V1.0 time-series tree cover product is now available at
278 <https://cstr.cn/31253.11.sciencedb.07173> (Yang and Zeng, 2023). This product is provided in the Mollweide
279 projection and the World Geodetic System 1984 (WGS1984) datum and geographic coordinate system. Tree
280 cover and non-tree cover are denoted as 0 and 1, respectively, in each yearly file, and are stored as UINT8 in
281 GeoTIFF format. The GeoTIFF files are named Planet-FC_SEA_<YEAR>_prj.tif, for example, Planet-
282 FC_SEA_16_prj.tif.

283

284 **6 Conclusions**

285 We have successfully generated the first accurate and high-resolution time-series tree cover map product for
286 SEA by combining optical and SAR satellite observations, utilizing advanced random forests machine
287 learning algorithms on the GEE platform. Our Planet-NICFI tree cover map products exhibit excellent
288 accuracy and consistency over six years (2016-2021). The baseline tree cover maps, with a resolution of 4.77
289 m, can be easily converted to forest cover maps at different resolutions to cater to the diverse needs of users.
290 Moreover, our tree cover products have the unique ability to address rounding errors in forest cover mapping
291 by accurately capturing isolated trees and monitoring the removal of long, narrow forest cover. These cutting-



292 edge fine-scale time-series tree cover maps represent a milestone in forest monitoring and offer
293 unprecedented opportunities for users across diverse disciplines.

294

295 **Code Availability**

296 The scripts used to generate all Planet-NICFI v1.0 tree cover 2016-2021 are provided in JavaScript
297 (https://code.earthengine.google.com/?scriptPath=users%2Fyftaurus%2Fcodes%3APlanet_RF-LC_rac).

298 The maps can be automatically generated by running the codes. The scripts are also available on request from
299 Z. Zeng.

300

301 **Acknowledgments**

302 This study was supported by the National Natural Science Foundation of China (grant no. 42071022), the
303 start-up fund provided by the Southern University of Science and Technology (no. 29/Y01296122), and the
304 China Postdoctoral Science Foundation (grant no. 2022M711472).

305

306 **Author contributions**

307 Z.Z. designed the research; F.Y. performed the analysis and wrote the draft. All authors contributed to the
308 interpretation of the results and the writing of the paper.

309

310 **Competing interests**

311 The authors declare no competing interests.



312 References

- 313 Achard, F., Beuchle, R., Mayaux, P. et al.: Determination of tropical deforestation rates and related carbon
314 losses from 1990 to 2010, *Glob Chang Biol*, 20(8), 2540-2554, 2014.
- 315 Brandt, M., Tucker, C. J., Kariryaa, A., et al.: An unexpectedly large count of trees in the West African Sahara
316 and Sahel, *Nature*, 587(7832), 78-82, 2020.
- 317 Buchhorn, M., Lesiv, M., Tsendbazar, N. E., et al.: Copernicus global land cover layers—collection 2, *Remote
318 Sens.*, 12(6), 1044, 2020.
- 319 Chen, J., Chen, J., Liao, A., et al.: Global land cover mapping at 30 m resolution: A POK-based operational
320 approach. *ISPRS J. Photogramm, Remote Sens.*, 103, 7-27, 2015.
- 321 CoP26, G. L.: Glasgow Leaders' Declaration on Forests and Land Use. Available online at: [https://ukcop26.
322 org/glasgow-leaders-declaration-on-forests-and-land-use/](https://ukcop26.org/glasgow-leaders-declaration-on-forests-and-land-use/)(accessed December 06, 2021).
- 323 ESA: Land Cover CCI Product User Guide Version 2. Tech. Rep. Available at:
324 maps.elie.ucl.ac.be/CCI/viewer/download/ESACCI-LC-Ph2-PUGv2_2.0.pdf, 2017.
- 325 FAO: Global forest resources assessment 2020: Main report. Technical report, Food and Agriculture
326 Organization of the United Nations, ROME, 2020.
- 327 Friedl, M., Sulla-Menashe, D.: MCD12Q1 MODIS/Terra+Aqua Land Cover Type Yearly L3 Global 500m
328 SIN Grid V006. NASA EOSDIS Land Processes DAAC. Accessed 2022-12-15 from
329 <https://doi.org/10.5067/MODIS/MCD12Q1.006>, 2019.
- 330 Gong P., Liu H., Zhang M., et al.: Stable classification with limited sample: Transferring a 30-m resolution
331 sample set collected in 2015 to mapping 10-m resolution global land cover in 2017, *Sci. Bull*, 64, 370-
332 373, 2019.
- 333 Gorelick, N., Hancher, M., Dixon, M., et al.: Google Earth Engine: Planetary-scale geospatial analysis for
334 everyone, *Remote Sens. Environ.*, 202, 18-27, 2017.
- 335 Hammer, D., Kraft, R., Wheeler, D.: Alerts of forest disturbance from MODIS imagery, *Int J Appl Earth Obs
336 Geoinf*, 33, 1-9, 2014.
- 337 Hansen, M. C., Potapov, P. V., Moore, R., et al.: High-resolution global maps of 21st-century forest cover
338 change, *Science*, 342(6160), 850-853, 2013.
- 339 Hansen, M. C., Stehman, S. V., Potapov, P. V.: Quantification of global gross forest cover loss, *Proc Natl
340 Acad Sci USA*, 107(19), 8650-8655, 2010.
- 341 Hsieh, P. F., Lee, L. C., Chen, N. Y.: Effect of spatial resolution on classification errors of pure and mixed
342 pixels in remote sensing, *IEEE Trans. Geosci. Remote Sens.*, 39(12), 2657-2663, 2001.
- 343 Karra K., Kontgis C., Statman-Weil Z., et al.: Global land use/land cover with Sentinel 2 and deep learning.
344 In 2021 IEEE international geoscience and remote sensing symposium IGARSS (pp. 4704-4707), IEEE,
345 2021, July.
- 346 Lang, N., Jetz, W., Schindler, K. Wegner, J. D.: A high-resolution canopy height model of the Earth,
347 [doi:10.48550/arxiv.2204.08322](https://doi.org/10.48550/arxiv.2204.08322), 2022.
- 348 Marta, S.: Planet imagery product specifications, Planet Labs: San Francisco, CA, USA, 91, 2018.
- 349 Mugabowindekwe, M., Brandt, M., Chave, J., et al.: Nation-wide mapping of tree-level aboveground carbon
350 stocks in Rwanda, *Nat. Clim. Change*, 1-7, 2023.
- 351 Oishi, Y., Sawada, Y., Kamei, A., et al.: Impact of Changes in Minimum Reflectance on Cloud Discrimination,
352 *Remote Sens.*, 10(5), 693, 2018.
- 353 Olofsson, P., Foody, G.M., Herold, M., et al.: Good practices for estimating area and assessing accuracy of
354 land change. *Remote Sens. Environ.* 148, 42-57, 2014.



- 355 Parker, C., Mitchell, A., Trivedi, M., Mardas, N.: The little REDD book: a guide to governmental and non-
356 governmental proposals for reducing emissions from deforestation and degradation. The little REDD
357 book: a guide to governmental and non-governmental proposals for reducing emissions from
358 deforestation and degradation,
359 http://www.globalcanopy.org/themedia/file/PDFs/LRB_lowres/lrb_en.pdf, 2008.
- 360 Planet Team: Planet Application Program Interface: In Space for Life on Earth. San Francisco, CA,
361 <https://api.planet.com>, 2017.
- 362 Reiner, F., Brandt, M., Tong, X., et al.: More than one quarter of Africa's tree cover found outside areas
363 previously classified as forest, 2022.
- 364 Roy, D.P., Huang, H., Houborg, R., Martins, V.S.: A global analysis of the temporal availability of
365 PlanetScope high spatial resolution multi-spectral imagery, *Remote Sens. Environ.*, 264, 112586, 2021.
- 366 Sexton, J.O., Noojipady, P., Song, X.P., Feng, M., Song, D.X., Kim, D.H., Anand, A., Huang, C., Channan,
367 S., Pimm, S.L., Townshend, J.R.: Conservation policy and the measurement of forests, *Nat. Clim.*
368 *Change*, 6(2), 192-196, 2016.
- 369 Shimada, M., Itoh, T., Motooka, T., Watanabe, M., Shiraishi, T., Thapa, R., & Lucas, R.: New global
370 forest/non-forest maps from ALOS PALSAR data (2007–2010), *Remote Sens. Environ.*, 155, 13-31,
371 2014.
- 372 Skea J., Shukla P. R., Reisinger A., et al.: Climate change 2022: Mitigation of climate change, IPCC Sixth
373 Assessment Report, 2022.
- 374 Tsendbazar, N., Herold, M., Li, L., et al.: Towards operational validation of annual global land cover maps,
375 *Remote Sens. Environ.*, 266, 112686, 2021.
- 376 Velasco, R.F., Lippe, M., Tamayo, F., et al.: Towards accurate mapping of forest in tropical landscapes: A
377 comparison of datasets on how forest transition matters, *Remote Sens. Environ.*, 274, 112997, 2022.
- 378 Wagner, F. H., Dalagnol, R., Silva-Junior, C. H., et al.: Mapping Tropical Forest Cover and Deforestation
379 with Planet NICFI Satellite Images and Deep Learning in Mato Grosso State (Brazil) from 2015 to 2021,
380 *Remote Sens.*, 15(2), 521, 2023.
- 381 Yang, F., Jiang, X., Ziegler, A. D., et al.: Improved fine-scale tropical forest cover mapping using Planet and
382 Sentinel-1 imagery, Unpublished, 2023.
- 383 Feng, Y., Ziegler, A. D., Elsen, P. R. et al.: Upward expansion and acceleration of forest clearance in the
384 mountains of Southeast Asia, *Nat. Sustain*, 4(10), 892-899, 2021.
- 385 Zanaga D., Van De Kerchove R., Daems D., et al.: ESA WorldCover 10 m 2021 v200,
386 <https://doi.org/10.5281/zenodo.7254221>, 2022.
- 387 Zanaga D., Van De Kerchove R., De Keersmaecker W., et al.: ESA WorldCover 10 m 2020 v100,
388 <https://doi.org/10.5281/zenodo.5571936>, 2021.
- 389 Zeng, Z., Estes, L., Ziegler, A. D., et al.: Highland cropland expansion and forest loss in Southeast Asia in
390 the twenty-first century, *Nat. Geosci*, 11(8), 556-562, 2018a.
- 391 Zeng, Z., Gower, D. and Wood, E. F.: Accelerating Forest loss in Southeast Asian Massif in the 21st century:
392 A case study in Nan Province, Thailand, *Glob Chang Biol*, 24, 4682-4695, 2018b.